

# Epitaxial growth of hybrid nanostructures

Tan, Chaoliang; Chen, Junze; Wu, Xue-Jun; Zhang, Hua

2018

Tan, C., Chen, J., Wu, X.-J., & Zhang, H. (2018). Epitaxial growth of hybrid nanostructures. *Nature Reviews Materials*, 3(2), 17089-. doi:10.1038/natrevmats.2017.89

<https://hdl.handle.net/10356/140484>

<https://doi.org/10.1038/natrevmats.2017.89>

---

© 2018 Macmillan Publishers Limited, part of Springer Nature. All rights reserved. This paper was published in *Nature Reviews Materials* and is made available with permission of Macmillan Publishers Limited, part of Springer Nature.

*Downloaded on 27 Aug 2022 12:33:19 SGT*

## **Epitaxial growth of hybrid nanostructures**

Chaoliang Tan, Junze Chen, Xue-Jun Wu and Hua Zhang\*

Center for Programmable Materials, School of Materials Science and Engineering,  
Nanyang Technological University, 50 Nanyang Avenue, Singapore 639798, Singapore

E-mail: [h Zhang@ntu.edu.sg](mailto:h Zhang@ntu.edu.sg)

Abstract | Hybrid nanostructures normally represent a class of materials composed of two or more different components, in which each component at least has one dimension at nanoscale. The rational design and controlled synthesis of hybrid nanostructures are of great importance to finely tune their properties and functions. Epitaxial growth promises a compelling way for the controlled synthesis of hybrid nanostructures with desired structures, crystal phases, exposed facets and/or interfaces. The aim of this Review Article is to provide a critical summary on the state-of-art progress made in the field of epitaxial growth of hybrid nanostructures. After the brief introduction, we will discuss the historic development, architectures and compositions, epitaxy methods, characterization techniques and advantages of epitaxial hybrid nanostructures sequentially. Moreover, we will also provide some personal discussion on challenges and future directions in this area on the basis of the current research status.

## **Introduction**

Hybrid nanostructures, as a class of functional nanomaterials, are composed of two or more distinctive components in which each component at least possesses one dimension at nanometer scale<sup>1-6</sup>. Hybrid nanostructures are potentially able to integrate the advantages and meanwhile overcome the weaknesses of individual components, thus realizing superior performances in some specific applications or even generating new properties and/or functions<sup>2,3</sup>. As known, the properties and functions of a hybrid nanostructure not only rely on its composition, but also depend on its structure, crystal phase, exposed facet, spatial organization, distribution of each component, and interface between components<sup>3</sup>. Therefore, the rational design and controlled synthesis of hybrid nanostructures is of particular importance not only in the realization of excellent performance towards specific applications, but also in fundamentally understanding the structure-correlated properties and functions.

Epitaxial growth promises a compelling way for the highly controlled synthesis of hybrid nanostructures with desired compositions, structures, crystal phases, exposed facets and interfaces<sup>7</sup>. Until now, a number of methods have been developed to achieve the epitaxial growth of hybrid nanostructures. For example, gas-phase epitaxy techniques, especially the chemical vapor deposition (CVD)<sup>8</sup>, have been widely used for the epitaxial growth of various hybrid nanostructures with controlled structures and compositions on various target substrates. Alternatively, solution-phase epitaxy methods, such as the colloidal synthesis and chemical reduction method, have also been developed for epitaxial growth of a wide range of hybrid nanostructures in high yield and large amount at relatively low cost<sup>7</sup>.

The last twenty years have witnessed the rapid development in the design and preparation of various kinds of epitaxial hybrid nanostructures with varying architectures and dimensionalities, such as core-shell nanostructures (e.g. zero-dimensional (0D) nanoparticles and nanopolyhedrons, one-dimensional (1D) nanorods and nanowires, two-dimensional (2D) nanoplates, nanoplatelets and nanosheets), nanoparticle-based hybrid nanostructures (e.g. nanoparticles decorated on other nanocrystals), well-defined heterostructures (e.g. core-crown nanoplatelets), hierarchical heterostructures (e.g. 1D nanorods grown on 2D nanoplates) and 2D/2D heterostructures (e.g. 2D lateral and vertical heterostructures), by using various epitaxy methods. These epitaxial nanostructures can be constructed from different compositions to form metal-metal, metal chalcogenide-metal chalcogenide, metal chalcogenide-metal oxide, metal-metal chalcogenide, metal-metal oxide and carbon-metal chalcogenide hybrids. Owing to the well-defined compositions, structures, crystal phases, exposed facets and/or interfaces enabled by the epitaxial growth, these epitaxial hybrid nanostructures have shown much enhanced performance in some specific applications, including electronics, optoelectronics and catalysis. In this Review Article, our aim is to give a critical overview on the state-of-art progress made in the field of epitaxial growth of hybrid nanostructures. After a brief introduction, we will retrospect the historic development in this field concisely. Then we will describe the various architectures of synthesized epitaxial hybrid nanostructures, followed by discussion on the methods used for preparation and the techniques used for characterization of epitaxial hybrid nanostructures. Thereafter, we will discuss the unique advantages of these epitaxial hybrid nanostructures in some applications, including electronics, optoelectronics and

catalysis. Finally, on the basis of the current research status, we will provide some personal insights on the challenges and the future research directions in this research area.

### **Historic development**

Epitaxial growth is a term used to define the deposition of one kind of crystalline materials on the well-defined surface of another crystalline substrate, in which the overgrown material has the same crystalline orientation with respect to the crystalline substrate<sup>9</sup>. The small lattice mismatch between two crystals is the key factor for the realization of their epitaxial growth, which can minimize the interface energy of hybrid nanostructures. The earliest study on the epitaxial growth of two crystals can be dated back to 1836 when Frankenheim reported the well-known result about the oriented deposition of sodium nitrate on calcite<sup>10</sup>. In 1928, Royer conducted extensive and systematic studies on a variety of materials by X-ray diffraction (XRD) in a more accurate way, which was able to study the effect of geometry of crystal orientation<sup>11</sup>. On the basis of his results, he first introduced the term “epitaxy” which means the “arrangement on” to describe such kind of growth mode between two crystals. Meanwhile, he also introduced two basic rules of epitaxy, i.e. (i) the orientated growth only occurs when the deposited crystalline material grows on the crystalline substrate that has an identical or quasi-identical crystalline structure and close lattice spacings, and (ii) the lattice mismatch between two crystals for the epitaxial growth should be less than 15%. The lattice mismatch was defined as  $(b-a)/a$ , where  $a$  and  $b$  are the corresponding lattice spacings of the crystalline substrate and deposited crystalline layer, respectively. The aforementioned general rules have been widely recognized by researchers to define the epitaxial growth between two crystals to date. Although the field of epitaxial growth

has been developed for about two centuries, early studies mainly focused on the epitaxial growth of big crystals or epitaxial deposition of thin films on single-crystalline bulk substrates<sup>9</sup>. The rising of research on epitaxial growth of hybrid nanostructures is along with the rapid development of synthesis of nanocrystals.

In 1990s when core-shell semiconductor quantum dots were synthesized, the study on epitaxial growth of hybrid nanostructures started. Although several groups reported the synthesis of core-shell semiconductor quantum dots, including CdSe@ZnS<sup>12</sup>, ZnSe@CdSe<sup>13</sup> and CdS@HgS@CdS<sup>14</sup>, the Alivisatos group first proposed and experimentally verified the epitaxial growth of CdS@HgS@CdS core-shell-shell<sup>15</sup> and CdSe@CdS core-shell<sup>16</sup> quantum dots in 1996 and 1997, respectively. Since then, researches on epitaxial growth of semiconductor core-shell or core-shell-shell quantum dots rapidly developed in the following decade. Significantly, the capability of synthesizing nanocrystals with well-defined facets (e.g. polyhedral nanoparticles) and anisotropies (e.g. nanorods, nanowires, nanoplates, nanoplatelets and nanosheets) offer great opportunities for the further epitaxial growth of another nanocrystal on their surface to construct well-defined heterostructures or more complex hybrid nanostructures. As a result, a variety of epitaxial hybrid nanostructures with varying compositions, structures, and architectures have been synthesized by various epitaxy methods. For example, inspired by core-shell quantum dots, a variety of epitaxial core-shell hybrid nanostructures in different structural forms, such as nanopolyhedrons<sup>17</sup>, nanorods<sup>18</sup>, nanowires<sup>19</sup>, nanoplates<sup>20</sup> and nanosheets<sup>21</sup>, have been synthesized. Furthermore, more complex or well-defined epitaxial hybrid nanostructures have also been reported. For example, semiconductor branched tetrapod heterostructures were

synthesized by a hot-injection method<sup>22</sup>. Well-defined heterostructured nanoplates, such as  $\text{Cu}_{1.94}\text{S-CdS}$  and  $\text{Cu}_{1.94}\text{S-Zn}_x\text{Cd}_{1-x}\text{S}$ , have been prepared via one-pot colloidal synthesis methods<sup>23</sup>. More importantly, the recently widely studied ultrathin 2D nanosheets provided an ideal platform for the epitaxial growth of well-defined hybrid nanostructures due to their single-crystalline nature and ultrathin thickness<sup>7</sup>. Since 2010, a variety of epitaxial hybrid nanostructures have been constructed based on ultrathin 2D nanosheets<sup>7</sup>. For example, nanoparticles and small nanoplates have been epitaxially grown on the surface of  $\text{MoS}_2$  to form hybrid nanostructures<sup>24</sup>. Moreover, 2D/2D lateral and vertical heterostructures have also been prepared by epitaxial growth of one kind of monolayer nanosheets from the edge site or on the top of the seed nanosheet<sup>7,8,25,26</sup>. Recently, the epitaxial growth of high-density semiconductor nanorods (e.g.  $\text{CdS}$  and  $\text{CdSe}$ ) on desired facets of 2D hexagonal-shaped  $\text{CuS}$ -derived nanoplates to form 1D/2D hierarchical heterostructures was also achieved by a colloidal synthesis method via seed engineering<sup>27</sup>. Promisingly, noble metals with unusual 4H phase, including Pt, Pd, Ir, Rh, Os and Ru, have been synthesized via the epitaxial growth by using the pre-synthesized ultrathin 4H Au nanoribbons as templates<sup>28</sup>. Based on the aforementioned description, the timeline of important research developments in the epitaxial growth of hybrid nanostructures is summarized in FIG. 1.

## **Architectures**

Until now, a wide spectrum of epitaxial hybrid nanostructures with varying architectures, dimensionalities and compositions, such as core-shell nanostructures, nanoparticle-based hybrid nanostructures, well-defined heterostructures, hierarchical heterostructures and 2D/2D heterostructures, have been prepared by various epitaxy methods. In this section,

we focus on introducing the types of structures and compositions of these synthesized epitaxial hybrid nanostructures, which are schematically shown in FIG. 2.

The core-shell nanostructure constructed by growing a layer of shell or multilayer shells on a seed nanocrystal is a typical architecture of epitaxial hybrid nanostructures (FIG. 2a). Typical examples include the epitaxial core-shell and core-shell-shell quantum dots which were first reported by Alivisatos and coworkers in late 1990s<sup>15,16</sup>. Since then, lots of epitaxial core-shell or core-shell-shell quantum dots with different sizes and compositions have been synthesized by using the similar methods<sup>29-44</sup>. Nanopolyhedrons, especially noble metal nanopolyhedrons, are another kind of widely reported epitaxial 0D core-shell nanostructures<sup>17,45,46</sup>. For example, Pt@Pd core-shell nanocubes, cuboctahedra and octahedra have been synthesized by epitaxial growth of Pd shells on highly faceted cubic Pt seeds<sup>17</sup>. Besides 0D nanostructures, 1D anisotropic core-shell nanostructures, such as nanorods<sup>18,47-49</sup>, nanowires<sup>19,50,51</sup> and nanoribbons<sup>52-55</sup>, with different compositions have also been constructed. For example, graded  $\text{Cd}_x\text{Zn}_{1-x}\text{S}$  shell was epitaxially grown on CdS nanorod to form core-shell nanorod<sup>18</sup>. As another important example, noble metals with unusual 4H phase have been successfully synthesized by using the pre-synthesized 4H Au nanoribbons as templates to form the core-shell nanoribbons through the epitaxial growth<sup>54</sup>. Besides 1D core-shell nanostructures, another typical type of anisotropic epitaxial core-shell hybrid nanostructures is 2D nanostructures, including nanoplates<sup>56</sup>, nanoplatelets<sup>57-60</sup> and nanosheets<sup>21,61</sup>. For example, semiconductor CdSe@CdS and CdSe@CdZnS core-shell nanoplatelets were prepared by epitaxial growth of CdS or CdZnS shell on the CdS nanoplatelet core<sup>56</sup>. In



addition, Au-based core-shell nanosheets can be constructed by the epitaxial growth of other noble metal shells, including Ag, Pt and Pd, on the ultrathin Au square sheets<sup>21,61</sup>.

Nanoparticle-based hybrid nanostructures are one important kind of epitaxial hybrid nanostructures, which are constructed by epitaxial deposition of spherical nanoparticles on the surface of other kinds of nanostructures, such as nanocubes<sup>62</sup>, nanooctahedra<sup>63</sup>, nanorods<sup>64</sup>, nanowires<sup>65,66</sup> and nanosheets<sup>24,67</sup> (FIG. 2b). For example, Pt-SrTiO<sub>3</sub> hybrid nanostructure was prepared by epitaxial growth of Pt nanoparticles on the surface of SrTiO<sub>3</sub> nanocubes<sup>62</sup>. In addition, nanoparticles can also be epitaxially grown on 1D nanorods and nanowires to form 0D/1D epitaxial hybrid nanostructures, such as Au-decorated CdSe nanorods<sup>64</sup>,  $\alpha$ -Fe<sub>2</sub>O<sub>3</sub> nanoparticle-decorated CdS nanowires<sup>65</sup> and CdS nanoparticle-decorated Bi<sub>2</sub>S<sub>3</sub> nanowires<sup>66</sup>. Furthermore, noble metal (e.g. Pt, Pd and Ag)<sup>24</sup> and PbSe<sup>67</sup> nanoparticles have also been epitaxially grown on 2D MoS<sub>2</sub> nanosheet to form epitaxial hybrid nanostructures.

Well-defined heterostructures, which are constructed by epitaxially aligning two nanocrystals together in an ordered manner, are another typical type of epitaxial hybrid nanostructures (FIG. 2c). For example, well-defined Cu<sub>1.94</sub>S-CdS and Cu<sub>1.94</sub>S-Zn<sub>x</sub>Cd<sub>1-x</sub>S heterostructures were prepared by epitaxial growth of Cu<sub>1.94</sub>S and CdS (or Zn<sub>x</sub>Cd<sub>1-x</sub>S) together, in which the Cu<sub>1.94</sub>S and CdS (or Zn<sub>x</sub>Cd<sub>1-x</sub>S) located at two sides to form hexagonal-shaped heterostructured nanoplates<sup>23</sup>. Similarly, well-defined Cu<sub>2</sub>S-PbS heterostructured nanocylinders can be built by growth of PbS semispherical tips on one side of Cu<sub>2</sub>S nanocubes<sup>68</sup>. Moreover, well-defined, screw-like, dumbbell-like and sandwich-like heterostructures have also been constructed from Cu<sub>1.94</sub>S and ZnS by finely tuning the experimental conditions<sup>69</sup>. Importantly, core-crown semiconductor

nanoplatelets, including CdSe-CdS<sup>70</sup> and CdSe-CdTe<sup>71</sup>, can be synthesized by laterally epitaxial growth of CdS or CdTe from the edge site of the CdSe nanoplatelet seed. In addition, well-defined dumbbell-like<sup>72</sup> and T-like Bi<sub>2</sub>Te<sub>3</sub>-Te<sup>73</sup> heterostructures have been constructed by epitaxial growth of Te nanoplates on two ends or one end of Bi<sub>2</sub>Te<sub>3</sub> nanorods, respectively. Moreover, nanoparticle dimer-like structures, including Au-Ag<sup>74</sup> and Au-Cu<sub>2</sub>ZnSnS<sub>4</sub><sup>75</sup>, are another type of well-defined epitaxial heterostructures. Impressively, single-layer transition metal dichalcogenide (TMD, e.g. WS<sub>2</sub> and MoS<sub>2</sub>) nanosheets have been epitaxially grown on one side of CdS nanoparticles to form well-defined heterostructures<sup>76</sup>.

Hierarchical heterostructures are one kind widely explored epitaxial hybrid nanostructures (FIG. 2d), which are normally established by epitaxial growth of 1D nanorods on the surfaces of nanoparticles, nanowires or nanoplates, or epitaxial growth of 2D nanoplates or nanosheets on 1D nanostructure surface. Branched heterostructures are the typical example of hierarchical heterostructures. For example, semiconductor branched tetrapod heterostructures can be constructed by epitaxial growth of CdTe nanorods on CdSe nanoparticles<sup>22</sup>. Similarly, branched ZnO-Ag and tetrapod CdS-Au heterostructures can also be constructed by epitaxial growth of ZnO nanorods on Ag truncated nanocubes<sup>77</sup> and CdS nanorods on Au nanoparticles<sup>78</sup>, respectively. Besides branched heterostructures, 1D/1D hierarchical heterostructures were constructed by vertically grown 1D nanowires on the backbone of 1D nanowires<sup>79-81</sup>. In addition, 2D/1D hierarchical heterostructures are another typical architecture of epitaxial hierarchical heterostructures. For example, 2D nanoplates or nanosheets are epitaxially grown on 1D nanostructures, such as Bi<sub>2</sub>Te<sub>3</sub> nanoplates vertically epitaxy on Te nanorods<sup>82</sup>, and edge

epitaxy of TMD nanosheets (e.g. MoS<sub>2</sub> and MoSe<sub>2</sub>) on Cu<sub>2-x</sub>S or CdS nanowires<sup>83</sup>. Alternatively, 1D nanorods can also be grown on 2D nanoplates to form 1D/2D hierarchical heterostructures. For example, nanorods or nanoneedles are epitaxially grown on 2D nanoplates, such as ZnO nanoneedles on Zn plates, and ZnO nanowires on CuGaO<sub>2</sub> nanoplates<sup>84</sup>. Impressively, high-density semiconductor nanorods (e.g. CdS and CdSe) have been epitaxially grown on desired facets of hexagonal-shaped 2D CuS-derived nanoplates selectively to form 1D/2D hierarchical heterostructures<sup>27</sup>.

2D/2D heterostructures are one type of epitaxial hybrid nanostructures which were extensively explored in recent years (FIG. 2e)<sup>3</sup>. 2D/2D heterostructures can be further classified into 2D lateral heterostructures and 2D vertical heterostructures. 2D lateral heterostructures are constructed by epitaxial growth of another kind of nanosheet from edge site of the seed nanosheet. For example, hexagonal boron nitride (*h*-BN) was epitaxially grown at the graphene edge to form single-layer graphene/*h*-BN lateral heterostructures<sup>85,86</sup>. Such kind of heterostructure has been extended to TMD heterostructures<sup>87-98</sup>. Interestingly, patterned arrays of 2D lateral heterostructures were also prepared by the selective conversion of one kind of 2D material to another under the assistance of masks<sup>99,100</sup>. Recently, 2D lateral TMD ternary heterostructures (A-B-C) and ordered heterostructures (A-B-A-B-A) have also been constructed by sequential growth of TMD monolayers laterally one by one in a controlled way<sup>101</sup>. 2D vertical heterostructures are built from the epitaxial growth of one kind of crystalline 2D nanosheet on the top of another. As known, graphene is a widely used 2D template for further epitaxial growth of other kinds of 2D nanosheets, such as topological insulators (e.g. Bi<sub>2</sub>Se<sub>3</sub> and In<sub>2</sub>Se<sub>3</sub>)<sup>102,103</sup>, TMDs (e.g. MoS<sub>2</sub>)<sup>104-108</sup> and MoC<sub>2</sub><sup>109</sup>, to form 2D vertical

heterostructures. Moreover, *h*-BN has also been used to support the epitaxial growth of graphene<sup>110-113</sup> and MoS<sub>2</sub><sup>114</sup> to form 2D vertical heterostructures. Lots of 2D TMD heterostructures have been prepared by epitaxial growth of one kind of TMD nanosheet onto another<sup>88,93,115-117</sup>. Moreover, 2D vertical heterostructures could also be constructed by epitaxial growth of metal sulfide nanoplates, including CuS, ZnS and Ni<sub>3</sub>S<sub>2</sub>, on the TiS<sub>2</sub> nanosheets<sup>118</sup>.

Understanding the underlying mechanisms or driving forces to form epitaxial hybrid nanostructures is very important. Taking the preparation of epitaxial heterostructures based on 0D seeds by the colloidal synthesis method as an example, lots of factors, such as the size and crystal structure of seeds, the lattice mismatch between seeds and second materials, the capping molecules and reaction temperature, can affect the final morphologies of the obtained heterostructures. Based on 0D seeds, high-quality epitaxial core-shell structures could be obtained, if the seeds and deposited second materials possess similar crystal structures with small lattice mismatch. In this case, the epitaxial growth of crystalline shell on another crystalline core can give rise to lower the total surface energy without generating significant interfacial stress, leading to the formation of core-shell nanostructures. If the overgrown material has a large lattice mismatch with the seed, the interface area between two crystal materials will tend to shrink in order to minimize the interfacial energy induced by the large lattice mismatch, resulting in the formation of nanodimers or the second nanostructure growing onto the seed (depending on the size of the seed and the diffusion ability of the second material)<sup>4</sup>. While further increasing the lattice mismatch, the second material tends to nucleate independently in the solution rather than on the surface of the seed<sup>30</sup>. Besides the lattice mismatch, the

capping molecules and the crystal structure of seeds can also affect the final morphologies of the obtained heterostructures. One typical example is the epitaxial growth of CdS-CdSe heterostructures by the colloidal synthesis method<sup>119</sup>. CdS with rod-like morphology can grow on the wurtzite CdSe seed in the presence of structure-directing molecule (e.g., phosphonic acid), while the nanotetrapod consisting of four CdS arms grown on CdSe core are obtained by using the zinc blende CdSe as seed<sup>119</sup>. The aforementioned principles might be used to explain the epitaxial growth of nanoparticle-based hybrid nanostructures, well-defined heterostructures and 2D/2D heterostructures. Although the matches of crystal structure, surface energies, capping molecules, and kinematic and thermodynamic modes have been proposed to explain the epitaxial growth of various hybrid nanostructures, there is still lack of a general model to explain the formation mechanism of epitaxial hybrid nanostructures with different morphologies, especially when they are prepared by different methods, i.e. CVD, chemical reduction, colloidal synthesis method, etc.

### **Epitaxy methods**

Until now, a number of synthetic methods, including the colloidal synthesis method, chemical reduction method, CVD, and so on, have been developed for the epitaxial growth of hybrid nanostructures. Each kind of method has its own advantage and disadvantage. In this section, we will discuss all the epitaxy methods used for epitaxial growth of hybrid nanostructures.

The colloidal synthesis method is widely used approach for the preparation of epitaxial metal chalcogenide hybrid nanostructures, including semiconductor core-shell quantum dots<sup>15,16</sup>, nanorods<sup>18,47,48</sup> and nanoplates<sup>58-60</sup>, and core-crown nanoplatelets<sup>70,71</sup>. The

colloidal synthesis method can be mainly divided into two types: hot-injection method and one-pot colloidal synthesis. Typically, the hot-injection method is to inject one kind of highly reactive reactants into a hot long-chain surfactant (e.g. oleyl amine and/or oleic acid) solution containing another kind of precursors at a given temperature. Then the mixed solution was heated up to an elevated temperature (up to 300 °C) for a certain time under an inert atmosphere to obtain target nanocrystals<sup>120</sup>. The epitaxial growth of hybrid nanostructures by the hot-inject method normally involves two steps, including the growth of seeded nanocrystals followed by the epitaxial growth of another kind nanostructures on them via a second step to form hybrid nanostructures<sup>15,16,18,47,48,58-60,70,71</sup>. Differently, the one-pot colloidal synthesis is to mix all precursors in a long-chain surfactant (e.g. oleyl amine and/or oleic acid) solution at room temperature to form a homogenous solution or slurry. Then the mixture was heated up to a higher temperature (up to 300 °C) to allow for the reaction of precursors for a certain time under an inert atmosphere to obtain epitaxial hybrid nanostructures<sup>23,3569,76</sup>. The colloidal synthesis allows for the controlled synthesis of colloidal epitaxial hybrid nanostructures with excellent mono-dispersity, uniform size, uniform shape and high purity, in which the size, shape, morphology, growth mode and architecture of synthesized epitaxial hybrid nanostructures can be finely tuned by tuning the experimental parameters, such as reaction temperature, reaction time, solvent system, type of precursors, concentration of precursors, and used surfactants or ligands. The compositions in synthesized epitaxial hybrid nanostructures can also be tuned via the post-synthetic cation or anion exchange reaction, in which their morphology can be still maintained<sup>83</sup>. Importantly, a recent study has demonstrated that the seed engineering is a compelling way to achieve the synthesis

of nanostructures on the desired facets of seed nanocrystals to obtain hierarchical heterostructures in a highly controlled manner<sup>27</sup>. The underlying mechanism for the selective epitaxial growth on different facets is still not very clear and needs to be further investigated.

In addition, the chemical reduction method has also been widely used for the epitaxial growth of metal-based hybrid nanostructures in solution<sup>121</sup>. The basic idea of this method is to grow one kind of metal shells or nanocrystals on another kind of metal cores or other nanostructure surfaces like metal oxides and metal chalcogenides via the chemical reduction of metal precursors by a proper reduction agent in the presence of surfactants. The growth rate and the lattice mismatch between the two crystals are the two key factors to achieve the epitaxial growth of hybrid nanostructures. Initially, this method was used to deposit a metal shell onto another metal nanocrystal to form core-shell nanostructures, especially noble metal core-shell nanostructures<sup>17,21,51-54,61</sup>. For example, by using Pt cubes as the seed, Pd shell can be epitaxially grown on the surface to form Pt@Pd core-shell cubes by reduction of  $K_2PdCl_4$  using ascorbic acid in an aqueous solution<sup>17</sup>. By introducing  $NO_2$  in the reaction to tune the growth rate, the shape of Pd cores can be finely tuned to obtain Pt@Pd core-shell cuboctahedra and octahedron<sup>17</sup>. The lattice mismatch between Pt and Pd is about 0.77%. Such small lattice mismatch allows for the epitaxial growth between them. However, when the same procedure was used to grow Au on Pt cube, non-epitaxial Pt-Au hybrid nanostructures composing of Pt cube partially embedded in the Au nanorod perimeter were obtained, instead of core-shell nanostructures due to the large lattice mismatch between Pt and Au ( $\sim 4.08\%$ )<sup>17</sup>. In another example, epitaxial Au@Ag core-shell square sheets were obtained by coating Ag

on the Au square sheet surface via the chemical reduction method due to the small lattice mismatch between Au and Ag ( $\sim 0.2\%$ )<sup>21</sup>. However, rhombic Au@Pt and Au@Pd nanoplates were obtained when Pt and Pd were coated on the Au square sheets due to the large lattice mismatch between Au and Pt or Pd ( $>5\%$ )<sup>61</sup>. Note that the phase transformation from the hcp to face-centered-cubic (fcc) phases of Au square sheets occurred during the further epitaxial growth of secondary metal on their surface<sup>21,61</sup>. This method is also effective for epitaxial deposition of metal nanocrystals on 2D nanosheets like MoS<sub>2</sub> to form epitaxial hybrid nanostructures<sup>24</sup>.

CVD, which has been proven to be a powerful method to grow nanomaterials including 2D materials<sup>122</sup>, is another widely used method for the epitaxial growth of hybrid nanostructures, especially 2D/2D heterostructures<sup>7,8</sup>. Briefly, the proper substrate placed in a furnace chamber is exposed to one or more airflow of gas and vapor precursors, which react and/or decompose on the substrate to obtain desired materials<sup>8,122</sup>. In most cases, the epitaxial growth of 2D/2D heterostructures involves the growth of 2D material seed followed by the further growth of secondary nanosheet on its top or at its edge to form 2D/2D vertical or lateral heterostructures, or selectively and partially transforming the seed material to another material to form patterned heterostructures<sup>7</sup>. Similarly, the crystal symmetry and lattice mismatch are two key factors to form epitaxial 2D/2D heterostructures. For example, graphene is easy to grow with *h*-BN sheets laterally or vertically to form *h*-BN-graphene lateral or vertical heterostructures since graphene has the same hexagonal symmetry as the *h*-BN with a close lattice distance<sup>85,86,110-113</sup>. Besides the *h*-BN, other 2D nanosheets, such as MoS<sub>2</sub><sup>104-108</sup> and MoC<sub>2</sub><sup>109</sup>, can also be epitaxially grown on graphene surface to form 2D vertical heterostructures via CVD methods. In



addition, a large number of 2D/2D TMD heterostructures have been prepared by epitaxial growth of one kind of TMD nanosheets on the top or at the edge site of another one owing to their same crystal symmetry and low lattice mismatch<sup>87-98,115-117</sup>. Patterned lateral 2D/2D TMD heterostructures, such as MoS<sub>2</sub>-MoSe<sub>2</sub> and WS<sub>2</sub>-WSe<sub>2</sub>, were obtained by combining the CVD method with lithography techniques, such as photolithography and electron beam lithography<sup>99,100</sup>. Besides binary 2D/2D heterostructures, 2D ternary heterostructures like WS<sub>2</sub>-WSe<sub>2</sub>-MoS<sub>2</sub> and WS<sub>2</sub>-MoSe<sub>2</sub>-WSe<sub>2</sub> and ordered heterostructures like WS<sub>2</sub>-WSe<sub>2</sub>-WS<sub>2</sub>-WSe<sub>2</sub>-WS<sub>2</sub> can also be prepared by sequentially epitaxial growth of these materials in a highly controlled manner via a step-by-step CVD process<sup>101</sup>. Apparently, CVD is a powerful and compelling technique for the epitaxial growth of heterostructures based on ultrathin 2D nanosheets in a highly controlled way. The controlled growth can be achieved by finely tuning the growth temperature, reaction time, concentration and rate of gas or vapor precursors, types of precursors, and substrates used. Note that the precursors used in CVD synthesis can be solids, mixed solid and gas, or gases. Based on the different precursors and target materials, the setup for CVD growth can be different from each other. It is worth pointing out that the CVD method also has its own disadvantages. For example, it normally needs harsh experimental conditions, such as high temperature and high vacuum, compared to solution-based epitaxy methods. Substrates are always indispensable, which are used to support the target materials grown in the CVD process. Therefore, additional process is required to transfer the synthesized materials for the further study or applications.

Physical vapor deposition (PVD) is another used method for the epitaxial growth of hybrid nanostructures, especially for the deposition of topological insulators on graphene

surface<sup>102,103</sup>. The basic idea is to evaporate a solid precursor (e.g.  $\text{Bi}_2\text{Se}_3$  or  $\text{In}_2\text{Se}_3$ ) to a vapor phase and then deposit it onto a target substrate predeposited with another kind of material (e.g. graphene) in a furnace to form vertical heterostructures<sup>102,103</sup>. The major difference between PVD and CVD is that there is no chemical reaction in PVD process. However, the advantages and disadvantages of PVD are quite similar to CVD.

Moreover, the electrochemical method has also been used for the epitaxial growth of hybrid nanostructures<sup>118</sup>. Its setup is similar to the Li-ion battery cell, in which the layered  $\text{TiS}_2$  crystal-coated metal foil (e.g. Cu, Zn and Ni) and Li foil were used as the cathode and anode, respectively<sup>118</sup>. A galvanostatic discharge process was then conducted to intercalate Li ions into  $\text{TiS}_2$  crystal to form Li-intercalated  $\text{TiS}_2$  compound<sup>118</sup>. The Li-intercalated  $\text{TiS}_2$  compound reacted with the metal foil slowly to achieve the epitaxial growth of metal sulfide nanoplates on the surface of  $\text{TiS}_2$  layers during the undisturbed period after the discharged process<sup>118</sup>. This method can achieve the epitaxial growth of 2D hybrid nanostructures in solution phase at room temperature. However, the procedure of this method is quite complicated and it takes long time (i.e. 2 weeks) to finish the reaction. Currently, how to extend this method for the epitaxial growth of other types of hybrid nanostructures is still under investigation.

In addition, the hydro/solvothermal method has been used for the epitaxial growth of hybrid nanostructures<sup>65,66,80</sup>. The precursors along with surfactants were first dissolved in water or organic solvent, and then the mixed solution was poured into a Teflon-lined steel autoclave reactor. The reactor was heated above the boiling point of the solvent to create high pressure inside the autoclave for facilitating the crystal growth. In order to form epitaxial hybrid nanostructures, pre-synthesized nanocrystals are dispersed in the solution

as the seed for the further epitaxial growth of another kind of materials on their surface. This simple hydro/solvothermal method is able to achieve the high-yield and large-scale synthesis of epitaxial hybrid nanostructures at relatively low temperature and low cost in solution phase. However, it is hard to realize highly controlled synthesis of uniform hybrid nanostructures. Besides the aforementioned methods, some other wet-chemical synthetic methods have also been developed for the epitaxial growth of hybrid nanostructures, such as the epitaxial growth of CuO on Ag nanowires<sup>50</sup>, ZnO nanorods on Ag nanocrystals<sup>77</sup> and ZnO nanorod arrays on CuGaO<sub>2</sub> nanoplates<sup>84</sup>.

### **Characterization techniques**

The rapid progress in nanoscience and nanotechnology has been driven by the great development of advanced characterization techniques. Finding and identifying reliable characterization techniques to prove epitaxial hybrid nanostructures is critically important to the further development of this research area. To date, a number of effective and powerful techniques, such as transmission electron microscope (TEM), scanning transmission electron microscope (STEM) and scanning tunneling microscope (STM), have been used to characterize the epitaxial growth of hybrid nanostructures. In this section, we will only focus on how to use these reliable techniques to characterize the epitaxial growth relationship in these hybrid nanostructures.

TEM is the most widely used tool to characterize the epitaxial growth of hybrid nanostructures. The most straightforward way is to visualize the lattice alignment at the interface of hybrid nanostructures in a high-resolution TEM (HRTEM) image, which can be used to see how the two different nanocrystals align together. The two different materials should have the same lattice orientation with close lattice distances if they are

epitaxially grown together. The HRTEM image at the interface area of hybrid nanostructures is most widely used to identify the epitaxial growth in most epitaxial hybrid nanostructures. For example, the HRTEM image of  $\text{Cu}_{1.94}\text{S}$ -CdS heterostructured nanoplates gave well aligned lattice fringes of the  $\text{Cu}_{1.94}\text{S}$  (800) planes and CdS (100) planes with a clear interface boundary (FIG. 3a), suggesting the epitaxial growth between  $\text{Cu}_{1.94}\text{S}$  and CdS<sup>23</sup>. Note that the HRTEM can only provide information on a limited area (a few  $\text{nm}^2$ ) in a image. Besides the HRTEM, selected area electron diffraction (SAED) pattern in TEM has also been widely used to identify the epitaxial growth. The SAED pattern of epitaxial hybrid nanostructures normally gives two sets of diffraction spots with the same symmetry, which are well aligned with each other without or with slight misorientation. The two sets of diffraction spots will overlap together and cannot be distinguished if the lattice distances of the two materials are too close. In contrast to the HRTEM, The SAED pattern can give information on a large area up to a few  $\mu\text{m}^2$ . Normally, the SAED pattern is combined with HRTEM images to verify the epitaxial growth of hybrid nanostructures. For example, the SAED pattern of CuS-TiS<sub>2</sub> hybrid nanostructures gives two sets of hexagonal shape diffraction spots, which are assignable to CuS nanoplates and TiS<sub>2</sub> nanosheets, respectively (FIG. 3b)<sup>118</sup>. The well alignment of two sets of diffraction spots without any misorientation proves the perfect epitaxial growth of CuS nanoplates on TiS<sub>2</sub> nanosheet surface<sup>118</sup>. Furthermore, the HRTEM image clearly shows the two well-aligned lattice fringes of the two crystals at the interface region (FIG. 3c)<sup>118</sup>. Both the SAED and HRTEM results confirmed the epitaxial growth between CuS and TiS<sub>2</sub>. Note that both SAED and HRTEM are also very useful to identify stacking faults and misorientations in epitaxial hybrid nanostructures. For example, the

percentage of epitaxially grown Pd nanoparticles can be calculated to be ~70% based on the HRTEM images, since not all the Pd nanoparticles are epitaxially grown on single-layer MoS<sub>2</sub> nanosheets<sup>24</sup>. Moreover, the six degree of misorientation can be also identified from the SAED pattern of triangular Ag nanoplates epitaxially grown on single-layer MoS<sub>2</sub> nanosheets<sup>24</sup>.

Although HRTEM image combining with SAED pattern in TEM is the most widely used way to identify the epitaxial growth of hybrid nanostructures in most reports, both of them in the common TEM mode cannot give information on spiral architectures and different atoms, making it difficult to identify the growth mode and boundary between different components. As known, in the high-angle annular dark field (HAADF)-STEM (HAADF-STEM) images, the atom contrast is directly proportional to the atomic number (Z) of the atom, thus allowing us to distinguish different atoms based on their contrast difference. Particularly, the HAADF-STEM imaging technique is able to discriminate and localize different atoms after introducing the optical aberration system. The HAADF-STEM imaging has been identified to be a powerful and compelling way to characterize the epitaxial growth of hybrid nanostructures, especially 2D/2D heterostructures. For example, the atomic resolution HAADF-STEM image of lateral WSe<sub>2</sub>-MoS<sub>2</sub> heterostructures at the interface area gives the single-crystal-like continuous lattice fringe without any grain boundary and misorientation (FIG. 3d), suggesting the epitaxial growth between monolayer WSe<sub>2</sub> and MoS<sub>2</sub> nanosheets<sup>90</sup>. The seamless interface and distinctive boundary of lateral WSe<sub>2</sub>-MoS<sub>2</sub> heterostructures shown in the atomic resolution HAADF-STEM image cannot be obtained in the normal HRTEM image<sup>90</sup>. Importantly, the distribution of Mo and W atoms is clearly observed since W atoms give brighter contrast

compared to Mo atoms<sup>90</sup>, allowing for identification of different atoms. Since the atomic resolution HAADF-STEM imaging technique is able to visualize the crystal growth and structure, and the different atoms in one image, it has been widely used to characterize 2D/2D heterostructures not only for identifying the epitaxial growth but also for characterizing other structural information like atom distribution, atom vacancies and doping of atoms. It is worth pointing out that it is much more complicated to get a good atomic-resolution HAADF-STEM image as compared to the HRTEM image and SAED pattern obtained in normal TEM. To date, this technology has been mainly used for the characterization of 2D/2D heterostructures. It is no doubt that it can be used for characterizing other kinds of epitaxial hybrid nanostructures. Of course, if it combines with other characterization techniques, more structural information on a hybrid nanostructure might be obtained.

STM is another useful technique to characterize the epitaxial growth of hybrid nanostructures. Similarly, STM can also provide lattice fringes at the interface area of hybrid nanostructures, thus identifying the epitaxial growth. However, STM has only been used for characterizing 2D/2D heterostructures recently. For example, the STM image of lateral *h*-BN-graphene heterostructure clearly shows the single-crystal-like lattice fringe at the interface area and the different contrast for *h*-BN and graphene (FIG. 3e), indicating their laterally epitaxial growth<sup>85</sup>. In addition, Moiré pattern can be clearly observed from the STM image of the vertical *h*-BN-graphene heterostructure due to the epitaxial growth (FIG. 3f), despite the presence of lattice mismatch between graphene and *h*-BN<sup>110</sup>.

It is worth pointing out that besides the aforementioned techniques, many others characterization techniques, such as XRD, X-ray photoelectron spectroscopy (XPS), Raman spectroscopy, photoluminescence, absorption spectroscopy, photoelectron spectroscopy and angle-resolved photoemission spectroscopy (ARPES), have also been widely used to characterize these epitaxial hybrid nanostructures to obtain some structural information, such as the chemical composition, size, thickness, hierarchical structure, optical property and photonic property. Although these aforementioned techniques have been used for characterization of other nanomaterials including 2D materials<sup>122</sup>, they have not been used to explore the epitaxial growth relationship in these hybrid nanostructures. Therefore, we will not discuss them in detail here.

### **Advantages in applications**

Previous studies have demonstrated that hybrid nanostructures normally exhibited much enhanced performances in some specific applications as compared to the individual components due to the synergistic effect between them no matter the growth mode, i.e. epitaxial or non-epitaxial growth. Therefore, it may wonder what the advantages of the epitaxial growth endowing with these epitaxial hybrid nanostructures are in applications. In this section, we will focus on discussion of the unique advantages of epitaxial hybrid nanostructures in some applications like electronics, optoelectronics and catalysis, in which their enhanced performances can be attributed to the epitaxial growth.

Epitaxial 2D/2D TMD heterostructures have been demonstrated to exhibit enhanced performances in electronics and optoelectronics as compared to the van der Waals heterostructures prepared by physically stacking the mechanically exfoliated TMD nanosheets together via polymer-assisted transfer methods. For example, the back-gating

field-effect transistor fabricated from the vertically epitaxial 2D/2D WS<sub>2</sub>-MoS<sub>2</sub> heterostructures exhibited a large ON/OFF ratio of >10<sup>6</sup> and high mobility of 15-34 cm<sup>2</sup> V<sup>-1</sup> s<sup>-1</sup> (Ref 88). The mobility is much higher than that of the vertically stacked WS<sub>2</sub>-MoS<sub>2</sub> heterostructures prepared by the polymer-assisted transfer method (0.51 cm<sup>2</sup> V<sup>-1</sup> s<sup>-1</sup>). It is believed that the much enhanced device performance is attributed to the clean interface enabled by the directly epitaxial growth, because the transfer method will introduce some contaminations trapped at the interface (FIG. 4a). Note that the 2D/2D lateral TMD heterostructures can be regarded as ideal p-n heterojunctions due to the well-defined *p*- or *n*-type characteristics of each component, making them promising fundamental platform for modern optoelectronics, including photodiodes. For example, the photodiode based on the lateral WSe<sub>2</sub>-WS<sub>2</sub> heterostructure exhibited a clear photovoltaic effect with an open-circuit voltage of ~0.47 V, short-circuit current of ~1.2 nA, and rapid temporal response faster than 100 μs under a laser illumination<sup>87</sup>. The calculated external and internal quantum efficiencies of the photon-to-electron conversion for the device are ~9.9% and ~43%, respectively<sup>87</sup>. The chemically bonded seamless interface of the lateral WSe<sub>2</sub>-WS<sub>2</sub> heterostructure enabled by the epitaxial growth might be mainly responsible to its high device performance (FIG. 4b).

Moreover, the epitaxial hybrid nanostructures have also been demonstrated to exhibit enhanced catalytic activities as compared to the non-epitaxial hybrid counterparts. For example, the CdS/α-Fe<sub>2</sub>O<sub>3</sub> epitaxial hybrid nanostructure exhibited superior photocatalytic activity toward the photodegradation of methylene blue compared to the non-epitaxial CdS/Fe<sub>3</sub>O<sub>4</sub> hybrid nanostructure<sup>65</sup>. It is suggested that the faster charge separation in the CdS/α-Fe<sub>2</sub>O<sub>3</sub> enabled by the epitaxial growth compared to the non-



epitaxial one is responsible to the much enhanced photocatalytic activity (FIG. 4c). Furthermore, the Pt-MoS<sub>2</sub> hybrid nanostructure composing of Pt nanoparticles epitaxially grown on MoS<sub>2</sub> nanosheets exhibited better electrocatalytic activity towards the hydrogen evolution reaction as compared to the commercial Pt/C catalyst<sup>24</sup>. The epitaxial growth-induced exposure of high-index facets is one of the main reasons for its excellent catalytic activity (FIG. 4d).

### **Conclusions and outlooks**

This Review Article summarized the state-of-art progress in the field of epitaxial growth of hybrid nanostructures. Until now, a large number of epitaxial hybrid nanostructures have been prepared by using different epitaxy methods, such as colloidal synthesis, chemical reduction method and CVD method. These epitaxial hybrid nanostructures can be built in forms of varying architectures with diverse components and dimensionalities. Based on the growth mode, these epitaxial hybrid nanostructures can be classified into five types, including core-shell nanostructures, nanoparticle-based hybrid nanostructures, well-defined heterostructures, hierarchical heterostructures, and 2D/2D heterostructures. To visualize the epitaxial growth of epitaxial hybrid nanostructures, a number of characterization techniques, such as TEM, STEM and STM, has been identified and used. Importantly, the epitaxial growth endowed these epitaxial hybrid nanostructures with some unique advantages, promising them great potential in a number of applications with enhanced performances, including electronics, optoelectronics and catalysis.

Although some achievements have been made, there are still some challenges remaining in this field. First, although a large number of epitaxial hybrid nanostructures have been synthesized, the controlled synthesis of epitaxial hybrid nanostructures with desired

components, structures, architectures and crystal phases still remains a big challenge. One possible way to achieve the highly controlled growth is to engineer the seeds used for epitaxial growth. A recent study has demonstrated that the seed engineering of 2D hexagonal-shaped nanoplates allows for the realization of highly controlled epitaxial growth of high-density semiconductor nanorod arrays on selective facets of 2D nanoplates to construct hierarchical heterostructures<sup>27</sup>. Such strategy might be used for epitaxial growth of other kinds of hybrid nanostructures in a highly controlled manner. Second, although a number of synthetic methods have been developed for epitaxial growth of hybrid nanostructures, the underlying mechanisms for the formation of these hybrid nanostructures still need to be fully understood. For example, by using in-situ characterization techniques, such as in-situ TEM<sup>123,124</sup>, the growth process of hybrid nanostructures can be in-situ monitored. Moreover, theoretical calculations can be conducted on the basis of the structure mode of these epitaxial hybrid nanostructures to provide some useful insights on the interface energy, which might help us to gain further understanding on the growth mechanism by combining the theoretical results with the experimental data. Third, another major challenge lies in the preparation of non-epitaxial hybrid nanostructures as comparison in order to explore the influence of the epitaxial growth on applications. As known, the performances of epitaxial hybrid nanostructures in some specific applications have been compared only with individual counterparts in most published results since it is difficult to prepare non-epitaxial hybrid nanostructures with similar structures used for comparison. The direct comparison of epitaxial and non-epitaxial hybrid nanostructures with similar structural characteristics in a given

application is of great important to verify the essential role of epitaxial growth in applications.

Although epitaxial growth of hybrid nanostructures has been studied more than twenty years, there is still much room for the further exploration and a lot of works can be done in the near future. From the material point of view, most of current epitaxial hybrid nanostructures are constructed from nanostructured semiconducting metal chalcogenides, TMDs, noble metals, graphene and *h*-BN. As known, there are many other widely explored nanomaterials, such as metal oxides, layered double hydroxides (LDHs), black phosphorus, metal-organic frameworks (MOFs), covalent-organic frameworks (COFs) and organic crystals, which possess diverse physical, chemical and electronic properties as well as wide potential applications<sup>122</sup>. Bearing this in mind, many new hybrid nanostructures might be constructed by epitaxial growth of one kind of these materials on or in another with controlled compositions, structures, and architectures, in which the lattice mismatch between two crystals needs to be considered and should be small. Moreover, nanostructured materials with new crystal phases might be synthesized through epitaxial growth by using pre-synthesized nanocrystals with unusual crystal phases as templates, since the coated crystals will follow the crystal lattice of the templates due to the epitaxial growth. Importantly, these nanostructures with new crystal phases might exhibit distinctive properties and functions as compared to those with common phases. On the other hand, from the application point of view, more efforts need to be devoted into understanding the role of epitaxial growth in properties and applications. Although some epitaxial hybrid nanostructures have shown better performances compared to the corresponding individual components in some given

applications, the performance of these epitaxial hybrid nanostructures have not been compared with the corresponding non-epitaxial nanostructures with similar structural features. Therefore, it is not clear how the epitaxial growth affects the performance since sometimes non-epitaxial hybrid nanostructures can also exhibit enhanced performances in many applications as compared to individual counterparts. In a word, in the near future, lots of effort could be devoted into this exciting research field in order to fulfill the ratio design, synthesis, characterization, property study, mechanism investigation, and promising applications of epitaxial hybrid nanostructures.

### **Acknowledgements**

This work was supported by MOE under AcRF Tier 2 (ARC 19/15, No. MOE2014-T2-2-093; MOE2015-T2-2-057; MOE2016-T2-2-103) and AcRF Tier 1 (2016-T1-001-147; 2016-T1-002-051), and NTU under Start-Up Grant (M4081296.070.500000) in Singapore. We would like to acknowledge the Facility for Analysis, Characterization, Testing and Simulation, Nanyang Technological University, Singapore, for use of their electron microscopy facilities.

Competing financial interests: The authors declare no competing financial interests.

### **References**

1. Costi, R., Saunders, A. E. & Banin, U. Colloidal hybrid nanostructures: A new type of functional materials. *Angew. Chem. Int. Ed.* **49**, 4878 (2010).
2. Huang, X., Tan, C., Yin, Z. & Zhang, H. 25th Anniversary Article: Hybrid nanostructures based on two-dimensional nanomaterials. *Adv. Mater.* **26**, 2185-2204 (2014).

3. Tan, C. & Zhang, H. Two-dimensional transition metal dichalcogenide nanosheet-based composites. *Chem. Soc. Rev.* **44**, 2713-2731 (2015).
4. Sun, Y. Interfaced heterogeneous nanodimers. *Natl. Sci. Rev.* **2**, 329-348 (2015).
5. Hu, Y. & Sun, Y. A generic approach for the synthesis of dimer nanoclusters and asymmetric nanoassemblies. *J. Am. Chem. Soc.* **135**, 2213-2221 (2013).
6. Hu, Y., Liu, Y., Li, Z. & Sun, Y. Highly asymmetric, interfaced dimers made of Au nanoparticles and bimetallic nanoshells: Synthesis and photo-enhanced catalysis. *Adv. Funct. Mater.* **24**, 2828-2836 (2014).
7. Tan, C. & Zhang, H. Epitaxial growth of hetero-nanostructures based on ultrathin two-dimensional nanosheets. *J. Am. Chem. Soc.* **137**, 12162-12174 (2015).
8. Li, H., Li, Y., Aljarb, A., Shi, Y. & Li, L.-J. Epitaxial growth of two-dimensional layered transition-metal dichalcogenides: Growth mechanism, controllability, and scalability. *Chem. Rev.* DOI: 10.1021/acs.chemrev.7b00212 (2017).
9. Matthews, J. W. in *Epitaxial growth* (Ed: Matthews, J. W.) (Academic Press, New York, 1975).
10. Frankenheim, M. L. Über die verbindung verschiedenartiger krystalle. *Ann. Phys.-Berlin* **113**, 516-522 (1836).
11. Royer, L. Experimental research on parallel growth on mutual orientation of crystals of different species. *Bull. Soc. Fr. Min.* **51**, 7-159 (1928).
12. Kortan, A. R. et al. Nucleation and growth of CdSe on ZnS quantum crystallite seeds, and vice versa, in inverse micelle media. *J. Am. Chem. Soc.* **112**, 1327-1332 (1990).
13. Hoener, C. F. et al. Demonstration of a shell-core structure in layered CdSe-ZnSe small particles by X-ray photoelectron and auger spectroscopies. *J. Phys. Chem.* **96**, 3812-3811 (1992).
14. Mews, A., Eychmiüller, A., Giersig, M., Schooss, D. & Weller, H. Preparation, characterization, and photophysics of the quantum dot quantum well system CdS/HgS/CdS. *J. Phys. Chem.* **98**, 934-941 (1994).
15. Mews, A., Kadavanich, A. V., Banin, U. & Alivisatos, A. P. Structural and spectroscopic investigations of CdS/HgS/CdS quantum-dot quantum wells. *Phys. Rev. B* **53**, 242-245 (1996).

16. Peng, X., Schlamp, M. C., Kadavanich, A. V. & Alivisatos, A. P. Epitaxial growth of highly luminescent CdSe/CdS core/shell nanocrystals with photostability and electronic accessibility. *J. Am. Chem. Soc.* **119**, 7019-7029 (1997).

**First example on the epitaxial growth, characterization and optical properties of CdSe/CdS core/shell quantum dots.**

17. Habas, S. E., Lee, H., Radmilovic, V., Somorjai, G. A. & Yang, P. Shaping binary metal nanocrystals through epitaxial seeded growth. *Nat. Mater.* **6**, 692-697 (2007).

**Epitaxial growth, characterization and electrocatalytic activity of noble metal core/shell polyhedral nanocrystals.**

18. Manna, L. Scher, E. C., Li, L.-S. & Alivisatos, A. P. Epitaxial growth and photochemical annealing of graded CdS/ZnS shells on colloidal CdSe nanorods. *J. Am. Chem. Soc.* **124**, 7136-7145 (2002).

19. Zhang, S. & Zeng, H. C. Solution-based epitaxial growth of magnetically responsive Cu@Ni nanowires. *Chem. Mater.* **22**, 1282-1284 (2010).

20. Lhuillier, E. *et al.* Two-dimensional colloidal metal chalcogenides semiconductors: Synthesis, spectroscopy, and applications. *Acc. Chem. Res.* **48**, 22-30 (2015).

21. Fan, Z. *et al.* Surface modification-induced phase transformation of hexagonal close-packed gold square sheets. *Nat. Commun.* **6**, 6571 (2015).

22. Milliron, D. J. *et al.* Colloidal nanocrystal heterostructures with linear and branched topology. *Nature* **430**, 190-195 (2004).

**Epitaxial growth and characterization of well-defined branch-like semiconductor heterostructures.**

23. Regulacio, M. D. *et al.* One-pot synthesis of Cu<sub>1.94</sub>S-CdS and Cu<sub>1.94</sub>S-Zn<sub>x</sub>Cd<sub>1-x</sub>S nanodisk heterostructures. *J. Am. Chem. Soc.* **133**, 2052-2055 (2011).

24. Huang, X. *et al.* Solution-phase epitaxial growth of noble metal nanostructures on dispersible single-layer molybdenum disulfide nanosheets. *Nat. Commun.* **4**, 1444 (2013).

**Epitaxial growth of noble metal nanocrystals on solution-dispersed single-layer MoS<sub>2</sub> nanosheets in solution phase.**

25. Chen, K., Wan, X. & Xu, J. Epitaxial stitching and stacking growth of atomically thin transition-metal dichalcogenides (TMDCs) heterojunctions. *Adv. Funct. Mater.* **27**, 1603884 (2017).
26. Tan, C., Lai, Z. & Zhang, H. Ultrathin two-dimensional multinary layered metal chalcogenide nanomaterials. *Adv. Mater.* **29**, 1701392 (2017).
27. Wu, X.-J., Chen, J., Tan, C., Zhu, Y., Han, Y. & Zhang, H. Controlled growth of high-density CdS and CdSe nanorod arrays on selective facets of two-dimensional semiconductor nanoplates. *Nat. Chem.* **8**, 470-475 (2016).  
**An example on highly-controlled epitaxial growth of high-density semiconductor nanorod arrays on selective facets of 2D semiconductor nanoplates via seed engineering.**
28. Fan, Z. & Zhang, H. Template synthesis of noble metal nanocrystals with unusual crystal structures and their catalytic applications. *Acc. Chem. Res.* **49**, 2841-2850 (2016).
29. Dabbousi, B. O. *et al.* (CdSe)ZnS core-shell quantum dots: Synthesis and characterization of a size series of highly luminescent nanocrystallites. *J. Phys. Chem. B* **101**, 9463-9475 (1997).
30. Cao, Y. & Banin, U. Growth and properties of semiconductor core/shell nanocrystals with InAs cores. *J. Am. Chem. Soc.* **122**, 9692-9702 (2000).
31. Talapin, D. V., Rogach, A. L., Kornowski, A., Haase, M. & Weller, H. Highly luminescent monodisperse CdSe and CdSe/ZnS nanocrystals synthesized in a hexadecylamine trioctylphosphine oxide trioctylphosphine mixture. *Nano Lett.* **1**, 207-211 (2001).
32. Malik, M. A., O'Brien, P. & Revaprasadu, N. A simple route to the synthesis of core/shell nanoparticles of chalcogenides. *Chem. Mater.* **14**, 2004-2010 (2002).
33. Cumberland, S. L. *et al.* Inorganic clusters as single-source precursors for preparation of CdSe, ZnSe, and CdSe/ZnS nanomaterials. *Chem. Mater.* **14**, 1576-1584 (2002).
34. Reiss, P., Bleuse, J. & Pron, A. Highly luminescent CdSe/ZnSe core/shell nanocrystals of low size dispersion. *Nano Lett.* **2**, 781-784 (2002).

35. Mekis, I., Talapin, D. V., Kornowski, A., Haase, M. & Weller, H. One-pot synthesis of highly luminescent CdSe/CdS core-shell nanocrystals via organometallic and “Greener” chemical approaches. *J. Phys. Chem. B* **107**, 7454-7462 (2003).
36. Li, J. *et al.* Large-scale synthesis of nearly monodisperse CdSe/CdS core/shell nanocrystals using air-stable reagents via successive ion layer adsorption and reaction. *J. Am. Chem. Soc.* **125**, 12567-12575 (2003).
37. Kim, S., Fisher, B., Eisler, H. & Bawendi, M. Type-II quantum dots: CdTe/CdSe(core/shell) and CdSe/ZnTe(core/shell) heterostructures. *J. Am. Chem. Soc.* **125**, 11466-11467 (2003).
38. Talapin, D. V., Mekis, I., Goltzinger, S., Kornowski, A., Benson, O. & Weller, H. CdSe/CdS/ZnS and CdSe/ZnSe/ZnS core-shell-shell nanocrystals. *J. Phys. Chem. B* **108**, 18826-18831 (2004).
39. Tsay, J. M., Pflughoeft, M., Bentolila, L. A. & Weiss, S. Hybrid approach to the synthesis of highly luminescent CdTe/ZnS and CdHgTe/ZnS nanocrystals. *J. Am. Chem. Soc.* **126**, 1926-1927 (2004).
40. Xie, R., Kolb, U., Li, J., Basche, T. & Mews, A. Synthesis and characterization of highly luminescent CdSe-Core CdS/Zn<sub>0.5</sub>Cd<sub>0.5</sub>S/ZnS multishell nanocrystals. *J. Am. Chem. Soc.* **127**, 7480-7488 (2005).
41. He, Y. *et al.* Microwave-assisted growth and characterization of water-dispersed CdTe/CdS core-shell nanocrystals with high photoluminescence. *J. Phys. Chem. B* **110**, 13370-13374 (2006).
42. Pan, D., Wang, Q., Jiang, S., Ji, X. & An, L. Synthesis of extremely small CdSe and highly luminescent CdSe/CdS core-shell nanocrystals via a novel two-phase thermal approach. *Adv. Mater.* **17**, 176-179 (2005).
43. Aharoni, A., Mokari, T., Popov, I. & Banin, U. Synthesis of InAs/CdSe/ZnSe core/shell1/shell2 structures with bright and stable near-infrared fluorescence. *J. Am. Chem. Soc.* **128**, 257-264 (2006).
44. Zhang, W., Chen, G., Wang, J., Ye, B. & Zhong, X. Design and synthesis of highly luminescent near-infrared-emitting water-soluble CdTe/CdSe/ZnS core/shell/shell quantum dots. *Inorg. Chem.* **48**, 9723-9731 (2009).



45. Fan, F. *et al.* Epitaxial growth of heterogeneous metal nanocrystals: From gold nano-octahedra to palladium and silver nanocubes. *J. Am. Chem. Soc.* **130**, 6949-6951 (2008).
46. Lu, C.-L., Prasad, K. S., Wu, H.-L., Ho, J. A. & Huang, M. H. Au nanocube-directed fabrication of Au-Pd core-shell nanocrystals with tetrahedral, concave octahedral, and octahedral structures and their electrocatalytic activity. *J. Am. Chem. Soc.* **132**, 14546-14553 (2010).
47. Talapin, D. V. *et al.* Highly emissive colloidal CdSe/CdS heterostructures of mixed dimensionality. *Nano Lett.* **3**, 1677-1681 (2003).
48. Mokari, T. & Banin, U. Synthesis and properties of CdSe/ZnS core/shell nanorods. *Chem. Mater.* **15**, 3955-3960 (2003).
49. Grzelczak, M., Rodríguez-González, B., Pérez-Juste, J. & Liz-Marzán, L. M. Quasi-epitaxial growth of Ni nanoshells on Au nanorods. *Adv. Mater.* **19**, 2262-2266 (2007).
50. Sciacca, B. *et al.* Solution-phase epitaxial growth of quasi-monocrystalline cuprous oxide on metal nanowires. *Nano Lett.* **14**, 5891-5898 (2014).
51. Niu, Z. *et al.* Ultrathin epitaxial Cu@Au core-shell nanowires for stable transparent conductors. *J. Am. Chem. Soc.* **139**, 7348-7354 (2017).
52. Fan, Z. *et al.* Stabilization of 4H hexagonal phase in gold nanoribbons. *Nat. Commun.* **6**, 7684 (2015).
53. Fan, Z. *et al.* Synthesis of 4H/fcc noble multimetallic nanoribbons for electrocatalytic hydrogen evolution reaction. *J. Am. Chem. Soc.* **138**, 1414-1419 (2016).
54. Fan, Z. *et al.* Epitaxial growth of unusual 4H hexagonal Ir, Rh, Os, Ru and Cu nanostructures on 4H Au nanoribbons. *Chem. Sci.* **8**, 795-799 (2017).
- Synthesis of noble metal shells with an unusual 4H phase on 4H Au nanoribbons via epitaxial growth.**
55. Huang, X., Wang, M., Shao, L., Willinger, M.-G., Lee, C.-S. & Meng, X.-M. Polarity-free epitaxial growth of heterostructured ZnO/ZnS core/shell nanobelts. *J. Phys. Chem. Lett.* **4**, 740-744 (2013).

56. Aherne, D., Charles, D. E., Brennan-Fournet, M. E., Kelly, J. M. & Gun'ko, Y. K. Etching-resistant silver nanoprisms by epitaxial deposition of a protecting layer of gold at the edges. *Langmuir* **25**, 10165-10173 (2009).
57. Mahler, B., Nadal, B., Bouet, C., Patriarche, G. & Dubertret, B. Core/shell colloidal semiconductor nanoplatelets. *J. Am. Chem. Soc.* **134**, 18591-18598 (2012).
58. Tessier, M. D., Mahler, B., Nadal, B., Heuclin, H., Pedetti, S. & Dubertret, B. Spectroscopy of colloidal semiconductor core/shell nanoplatelets with high quantum yield. *Nano Lett.* **13**, 3321-3328 (2013).
59. Kunneman, L. T. *et al.* Bimolecular auger recombination of electron-hole pairs in two-dimensional CdSe and CdSe/CdZnS core/shell nanoplatelets. *J. Phys. Chem. Lett.* **4**, 3574-3578 (2013).
60. Bouet, C. *et al.* Synthesis of zinc and lead chalcogenide core and core/shell nanoplatelets using sequential cation exchange reactions. *Chem. Mater.* **26**, 3002-3008 (2014).
61. Fan, Z. *et al.* Synthesis of ultrathin face-centered-cubic Au@Pt and Au@Pd core-shell nanoplates from hexagonal-close-packed Au square sheets. *Angew. Chem. Int. Ed.* **54**, 5672-5676 (2015).
62. Enterkin, J. A., Poeppelmeier, K. R. & Marks, L. D. Oriented catalytic platinum nanoparticles on high surface area strontium titanate nanocuboids. *Nano Lett.* **11**, 993-997 (2011).
63. Sneed, B. T., Kuo, C.-H., Brodsky, C. N. & Tsung, C.-K. Iodide-mediated control of rhodium epitaxial growth on well-defined noble metal nanocrystals: Synthesis, characterization, and structure-dependent catalytic properties. *J. Am. Chem. Soc.* **134**, 18417-18426 (2012).
64. Figuerola, A. *et al.* Epitaxial CdSe-Au nanocrystal heterostructures by thermal annealing. *Nano Lett.* **10**, 3028-3036 (2010).
65. Wang, L., Wei, H., Fan, Y., Gu, X. & Zhan, J. One-dimensional CdS/ $\alpha$ -Fe<sub>2</sub>O<sub>3</sub> and CdS/Fe<sub>3</sub>O<sub>4</sub> heterostructures: Epitaxial and nonepitaxial growth and photocatalytic activity. *J. Phys. Chem. C* **113**, 14119-14125 (2009).

66. Fang, Z. *et al.* Epitaxial growth of CdS nanoparticle on Bi<sub>2</sub>S<sub>3</sub> nanowire and photocatalytic application of the heterostructure. *J. Phys. Chem. C* **115**, 13968-13976 (2011).
67. Schornbaum, J. *et al.* Epitaxial growth of PbSe quantum dots on MoS<sub>2</sub> nanosheets and their near-infrared photoresponse. *Adv. Funct. Mater.* **24**, 5798-5806 (2014).
68. Zhuang, T., Fan, F., Gong, M. & Yu, S. Cu<sub>1.94</sub>S nanocrystal seed mediated solution-phase growth of unique Cu<sub>2</sub>S-PbS heteronanostructures. *Chem. Commun.* **48**, 9762-9764 (2012).
69. Han, S., Gong, M., Yao, H., Wang, Z. & Yu, S. One-pot controlled synthesis of hexagonal-prismatic Cu<sub>1.94</sub>S-ZnS, Cu<sub>1.94</sub>S-ZnS-Cu<sub>1.94</sub>S, and Cu<sub>1.94</sub>S-ZnS-Cu<sub>1.94</sub>S-ZnS-Cu<sub>1.94</sub>S heteronanostructures. *Angew. Chem. Int. Ed.* **51**, 6365-6368 (2012).
70. Tessier, M. D. *et al.* Efficient exciton concentrators built from colloidal core/crown CdSe/CdS semiconductor nanoplatelets. *Nano Lett.* **14**, 207-213 (2014).
71. Pedetti, S., Ithurria, S., Heuclin, H., Patriarche, G. & Dubertret, B. Type-II CdSe/CdTe core/crown semiconductor nanoplatelets. *J. Am. Chem. Soc.* **136**, 16430-16438 (2014).
72. Wang, W. *et al.* Epitaxial growth of shape-controlled Bi<sub>2</sub>Te<sub>3</sub>-Te heterogeneous nanostructures. *J. Am. Chem. Soc.* **132**, 17316-17324 (2010).
73. Cheng, L. *et al.* T-shaped Bi<sub>2</sub>Te<sub>3</sub>-Te heteronanojunctions: Epitaxial growth, structural modeling, and thermoelectric properties. *J. Phys. Chem. C* **117**, 12458-12464 (2013).
74. Sun, Y., Foley, J. J., Peng, S., Li, Z. & Gray, S. K. Interfaced metal heterodimers in the quantum size regime. *Nano Lett.* **13**, 3958-3964 (2013).
75. Patra, B. K. *et al.* Coincident site epitaxy at the junction of Au-Cu<sub>2</sub>ZnSnS<sub>4</sub> heteronanostructures. *Chem. Mater.* **27**, 650-657 (2015).
76. Chen, J. *et al.* One-pot synthesis of CdS nanocrystals hybridized with single-layer transition-metal dichalcogenide nanosheets for efficient photocatalytic hydrogen evolution. *Angew. Chem. Int. Ed.* **54**, 1210-1214 (2015).
77. Fan, F., Ding, Y., Liu, D., Tian, Z. & Wang, Z. L. Facet-selective epitaxial growth of heterogeneous nanostructures of semiconductor and metal: ZnO nanorods on Ag nanocrystals. *J. Am. Chem. Soc.* **131**, 12036-12037 (2009).

78. Halder, K. K., Pradhan, N. & Patra, A. Formation of heteroepitaxy in different shapes of Au-CdSe metal-semiconductor hybrid nanostructures. *Small* **9**, 3424-3432 (2013).
79. Zhou, W. *et al.* Controllable fabrication of high-quality 6-fold symmetry-branched CdS nanostructures with ZnS nanowires as templates. *J. Phys. Chem. C* **112**, 9253-9260 (2008).
80. Zhou, W. *et al.* Epitaxial growth of branched  $\alpha$ -Fe<sub>2</sub>O<sub>3</sub>/SnO<sub>2</sub> nano-heterostructures with improved lithium-ion battery performance. *Adv. Funct. Mater.* **21**, 2439-2445 (2011).
81. An, H. *et al.* Unusual Rh nanocrystal morphology control by hetero-epitaxially growing Rh on Au@Pt nanowires with numerous vertical twinning boundaries. *Nanoscale* **7**, 8309-8314 (2015).
82. Lu, W., Ding, Y., Chen, Y., Wang, Z. L. & Fang, J. Bismuth telluride hexagonal nanoplatelets and their two-step epitaxial growth. *J. Am. Chem. Soc.* **127**, 10112-10116 (2005).
83. Chen, J. *et al.* Edge epitaxy of two-dimensional MoSe<sub>2</sub> and MoS<sub>2</sub> nanosheets on one-dimensional nanowires. *J. Am. Chem. Soc.* **139**, 8653-8660 (2017).
84. Forticaux, A., Hacialioglu, S., DeGrave, J. P., Dziejczak, R. & Jin, S. Three-dimensional mesoscale heterostructures of ZnO nanowire arrays epitaxially grown on CuGaO<sub>2</sub> nanoplates as individual diodes. *ACS Nano* **7**, 8224-8232 (2013).
85. Liu, L. *et al.* Heteroepitaxial growth of two-dimensional hexagonal boron nitride templated by graphene edges. *Science* **343** 163-167 (2014).
- Epitaxial growth of hexagonal boron nitride on graphene edges to form lateral heterostructures.**
86. Shin, H.-C. *et al.* Epitaxial growth of a single-crystal hybridized boron nitride and graphene layer on a wide-band gap semiconductor. *J. Am. Chem. Soc.* **137**, 6897-6905 (2015).
87. Duan, X., *et al.* Lateral epitaxial growth of two-dimensional layered semiconductor heterojunctions. *Nat. Nanotechnol.* **9**, 1024-1030 (2014).
- Epitaxial growth of monolayer transition metal dichalcogenide lateral heterostructures.**

88. Gong, Y. *et al.* Vertical and in-plane heterostructures from WS<sub>2</sub>/MoS<sub>2</sub> monolayers. *Nat. Mater.* **13**, 1135-1142 (2014).  
**Epitaxial growth of monolayer transition metal dichalcogenide lateral and vertical heterostructures.**
89. Huang, C. *et al.* Lateral heterojunctions within monolayer MoSe<sub>2</sub>-WSe<sub>2</sub> semiconductors. *Nat. Mater.* **13**, 1096-1101 (2014).
90. Li, M.-Y. *et al.* Epitaxial growth of a monolayer WSe<sub>2</sub>-MoS<sub>2</sub> lateral p-n junction with an atomically sharp interface. *Science* **349**, 524-528 (2015).  
**Epitaxial growth of monolayer transition metal dichalcogenide lateral p-n heterojunctions with an atomically sharp interface.**
91. Chen, J. *et al.* Lateral epitaxy of atomically sharp WSe<sub>2</sub>/WS<sub>2</sub> heterojunctions on silicon dioxide substrates. *Chem. Mater.* **28**, 7194-7197 (2016).
92. Yu, Y. *et al.* Equally efficient interlayer exciton relaxation and improved absorption in epitaxial and nonepitaxial MoS<sub>2</sub>/WS<sub>2</sub> heterostructures. *Nano Lett.* **15**, 486-491 (2015).
93. Yoo, Y., Degregorio, Z. P. & Johns, J. E. Seed crystal homogeneity controls lateral and vertical heteroepitaxy of monolayer MoS<sub>2</sub> and WS<sub>2</sub>. *J. Am. Chem. Soc.* **137**, 14281-14287 (2015).
94. Zhang, X.-Q., Lin, C.-H., Tseng, Y.-W., Huang, K.-H. & Lee, Y.-H. Synthesis of lateral heterostructures of semiconducting atomic layers. *Nano Lett.* **15**, 410-415 (2015).
95. Chen, K. *et al.* Lateral built-in potential of monolayer MoS<sub>2</sub>-WS<sub>2</sub> in-plane heterostructures by a shortcut growth strategy. *Adv. Mater.* **27**, 6431-6437 (2015).
96. Chen, K. *et al.* Electronic properties of MoS<sub>2</sub>-WS<sub>2</sub> heterostructures synthesized with two-step lateral epitaxial strategy. *ACS Nano* **9**, 9868-9876 (2015).
97. Li, H. *et al.* Composition modulated two-dimensional semiconductor lateral heterostructures via layer-selected atomic substitution. *ACS Nano* **11**, 961-967 (2017).
98. Bogaert, K. *et al.* Diffusion-mediated synthesis of MoS<sub>2</sub>/WS<sub>2</sub> lateral heterostructures. *Nano Lett.* **16**, 5129-5134 (2016).

99. Mahjouri-Samani, M. *et al.* Patterned arrays of lateral heterojunctions within monolayer two-dimensional semiconductors. *Nat. Commun.* **6**, 7749 (2015).
100. Li, H. *et al.* Laterally stitched heterostructures of transition metal dichalcogenide: Chemical vapor deposition growth on lithographically patterned area. *ACS Nano* **10**, 10516-10523 (2016).
101. Zhang, Z., Chen, P., Duan, X., Zang, K., Luo, J. & Duan, X. Robust epitaxial growth of two-dimensional heterostructures, multiheterostructures, and superlattices. *Science* **357**, 788-792 (2017).
102. Dang, W., Peng, H., Li, H., Wang, P. & Liu, Z. Epitaxial heterostructures of ultrathin topological insulator nanoplate and graphene. *Nano Lett.* **10**, 2870-2876 (2010).
103. Lin, M. *et al.* Controlled growth of atomically thin In<sub>2</sub>Se<sub>3</sub> flakes by van der Waals epitaxy. *J. Am. Chem. Soc.* **135**, 13274-13277 (2013).
104. Shi, Y. *et al.* van der Waals epitaxy of MoS<sub>2</sub> layers using graphene as growth templates. *Nano Lett.* **12**, 2784-2791 (2012).
105. Lin, Y.-C. *et al.* Direct synthesis of van der Waals solids. *ACS Nano* **8**, 3715-3723 (2014).
106. Azizi, A. *et al.* Freestanding van der Waals heterostructures of graphene and transition metal dichalcogenides. *ACS Nano* **9**, 4882-4890 (2015).
107. Liu, X. *et al.* Rotationally commensurate growth of MoS<sub>2</sub> on epitaxial graphene. *ACS Nano* **10**, 1067-1075 (2016).
108. Ago, H. *et al.* Visualization of grain structure and boundaries of polycrystalline graphene and two-dimensional materials by epitaxial growth of transition metal dichalcogenides. *ACS Nano* **10**, 3233-3240 (2016).
109. Xu, C. *et al.* Strongly coupled high-quality graphene/2D superconducting Mo<sub>2</sub>C vertical heterostructures with aligned orientation. *ACS Nano* **11**, 5906-5914 (2017).
110. Yang, W. *et al.* Epitaxial growth of single-domain graphene on hexagonal boron nitride. *Nat. Mater.* **12**, 792-797 (2013).
111. Gao, T. *et al.* Temperature-triggered chemical switching growth of in-plane and vertically stacked graphene-boron nitride heterostructures. *Nat. Commun.* **6**, 6835 (2015).

112. Zhang, C. *et al.* Direct growth of large-area graphene and boron nitride heterostructures by a co-segregation method. *Nat. Commun.* **6**, 6519 (2015).
113. Li, Q. *et al.* Nickelocene-precursor-facilitated fast growth of graphene/h-BN vertical heterostructures and its applications in OLEDs. *Adv. Mater.* **29**, 1701325 (2017).
114. Fu, D. *et al.* Molecular beam epitaxy of highly-crystalline monolayer molybdenum disulfide on hexagonal boron nitride. *J. Am. Chem. Soc.* **139**, 9392-9400 (2017).
115. Ionescu, R. *et al.* Two step growth phenomena of molybdenum disulfide-tungsten disulfide heterostructures. *Chem. Commun.* **51**, 11213-11216 (2015).
116. Woods, J. M. *et al.* One-step synthesis of MoS<sub>2</sub>/WS<sub>2</sub> layered heterostructures and catalytic activity of defective transition metal dichalcogenide films. *ACS Nano* **10**, 2004-2009 (2016).
117. Shi, J. *et al.* Temperature-mediated selective growth of MoS<sub>2</sub>/WS<sub>2</sub> and WS<sub>2</sub>/MoS<sub>2</sub> vertical stacks on Au foils for direct photocatalytic applications. *Adv. Mater.* **28**, 10664-10672 (2016).
118. Tan, C. *et al.* Liquid-phase epitaxial growth of two-dimensional semiconductor hetero-nanostructures. *Angew. Chem. Int. Ed.* **54**, 1841-1845 (2015).
119. Talapin, D. V., Nelson, J. H., Shevchenko, E. V., Aloni, S., Sadtler, B., Alivisatos, A. P. Seeded growth of highly luminescent CdSe/CdS nanoheterostructures with rod and tetrapod morphologies. *Nano Lett.* **7**, 2951-2959 (2007).
120. Murray, C. B., Norris, D. J. & Bawendi, M. G. Synthesis and characterization of nearly monodisperse Cde (E = S, Se, Te) semiconductor nanocrystallites. *J. Am. Chem. Soc.* **115**, 8706-8715 (1993).
121. Xia, Y., Xiong, Y., Lim, B. & Skrabalak, S. E. Shape-controlled synthesis of metal nanocrystals: Simple chemistry meets complex physics? *Angew. Chem. Int. Ed.* **48**, 60-103 (2009).
122. Tan, C. *et al.* Recent advances in ultrathin two-dimensional nanomaterials. *Chem. Rev.* **117**, 6225-6331 (2017).
123. Zeng, Z., Zheng, W. & Zheng, H. Visualization of colloidal nanocrystal formation and electrode-electrolyte interfaces in liquids using TEM. *Acc. Chem. Res.* **50**, 1808-1817 (2017).

124. Wang, S. *et al.* In situ atomic-scale studies of the formation of epitaxial Pt nanocrystals on monolayer molybdenum disulfide. *ACS Nano* **11**, 9057-9067 (2017).





**Figure 1 | Timeline showing some important developments in the epitaxial growth of hybrid nanostructures.**

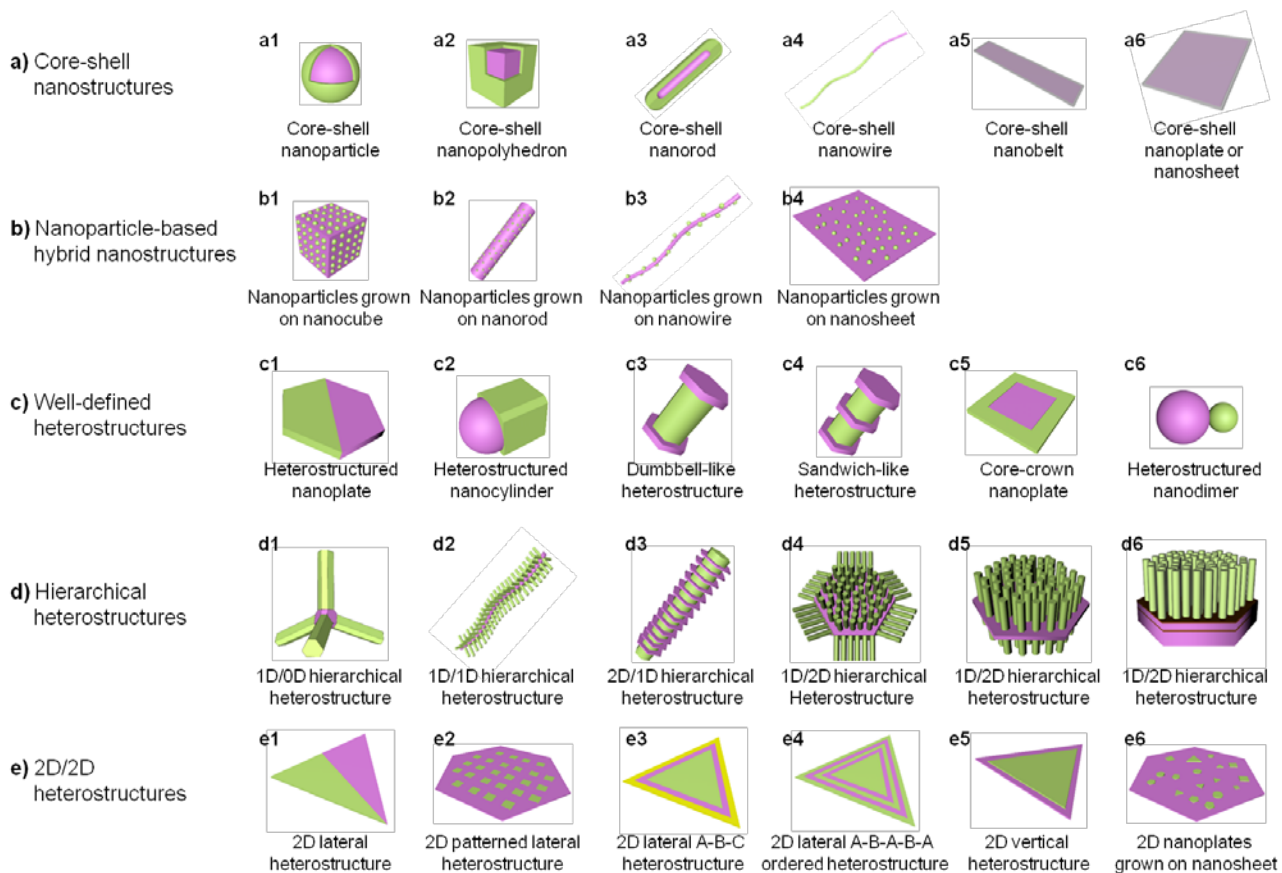


**Figure 2 | Schematic illustration of typical architectures of epitaxial hybrid nanostructures.** (a) Epitaxial core-shell nanostructures, including quantum dots, nanopolyhedrons, nanorods, nanowires, nanobelts, and nanoplates or nanosheets. (b) Epitaxial nanoparticle-based hybrid nanostructures, including nanoparticles grown on nanocubes, nanorods, nanowires, and nanosheets. (c) Epitaxial well-defined heterostructures, including heterostructured nanodimers, heterostructured nanocylinders, dumbbell-line heterostructures, sandwich-like heterostructures, heterostructured nanoplates, and core-crown nanoplates. (d) Epitaxial hierarchical heterostructures, including 1D/0D hierarchical heterostructures, 1D/1D hierarchical heterostructures, 2D/1D hierarchical heterostructures and 1D/2D hierarchical heterostructures. (e) Epitaxial 2D/2D heterostructures, including 2D lateral heterostructures, 2D patterned lateral heterostructures, 2D ternary A-B-C lateral heterostructures, 2D A-B-A-B-A ordered heterostructures, 2D nanoplates grown on nanosheets, and 2D vertical heterostructures.

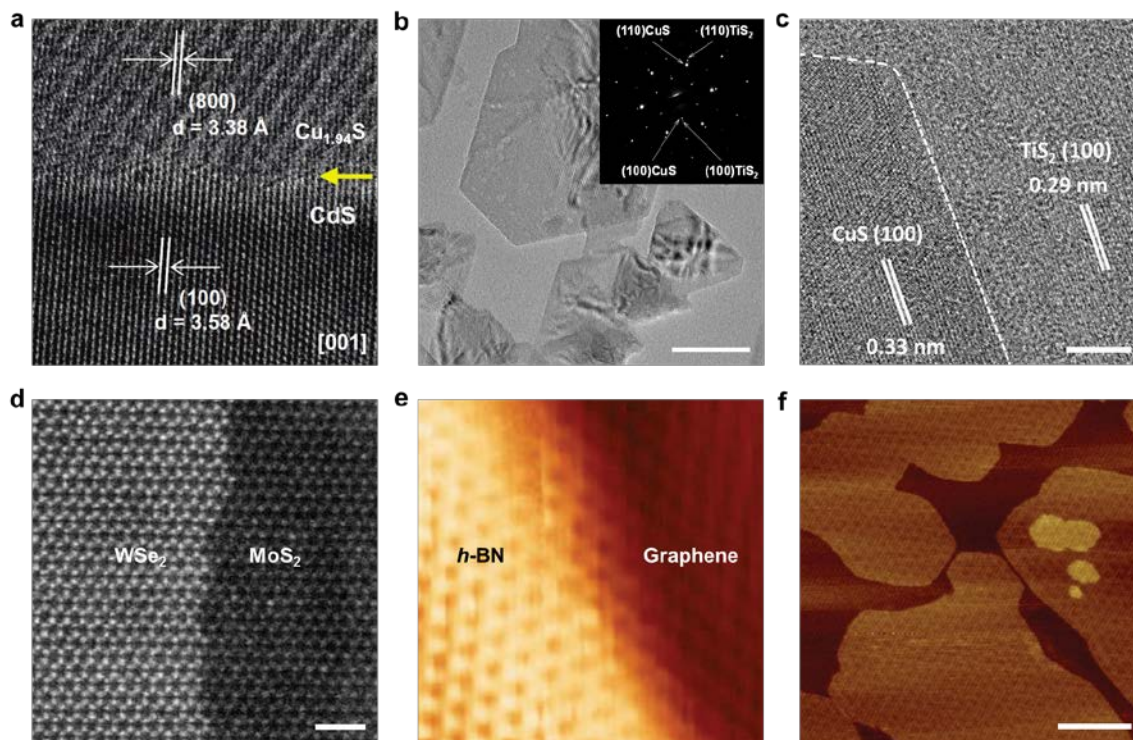


**Figure 3 | Characterization of epitaxial hybrid nanostructures.** (a) HRTEM image of  $\text{Cu}_{1.94}\text{S}$ -CdS heterostructured nanoplates at the interface area. The yellow arrow indicates the interface boundary between  $\text{Cu}_{1.94}\text{S}$  and CdS. Adapted, with permission, from ref. 23 (copyright 2011 American Chemical Society). (b) TEM image of 2D CuS-TiS<sub>2</sub> heterostructures (Scale bar, 50 nm). Inset: The corresponding SAED pattern. (c) HRTEM image of 2D CuS-TiS<sub>2</sub> heterostructure at the interface area (Scale bar, 2 nm). Adapted, with permission, from ref. 118 (copyright 2015 John Wiley & Sons Inc). (d) Atomic-resolution HAADF-STEM image of WSe<sub>2</sub>-MoS<sub>2</sub> lateral heterostructures at the interface area (Scale bar, 1 nm). Adapted, with permission, from ref. 90 (copyright 2015 AAAS). (e) Atomic-resolution STM image of *h*-BN-graphene lateral heterostructures at the interface area. Adapted, with permission, from ref. 85 (copyright 2014 AAAS). (f) Moiré pattern of *h*-BN-graphene vertical heterostructures observed in a STM image (Scale bar, 100 nm). Adapted, with permission, from ref. 110 (copyright 2013 Nature Publishing Group).

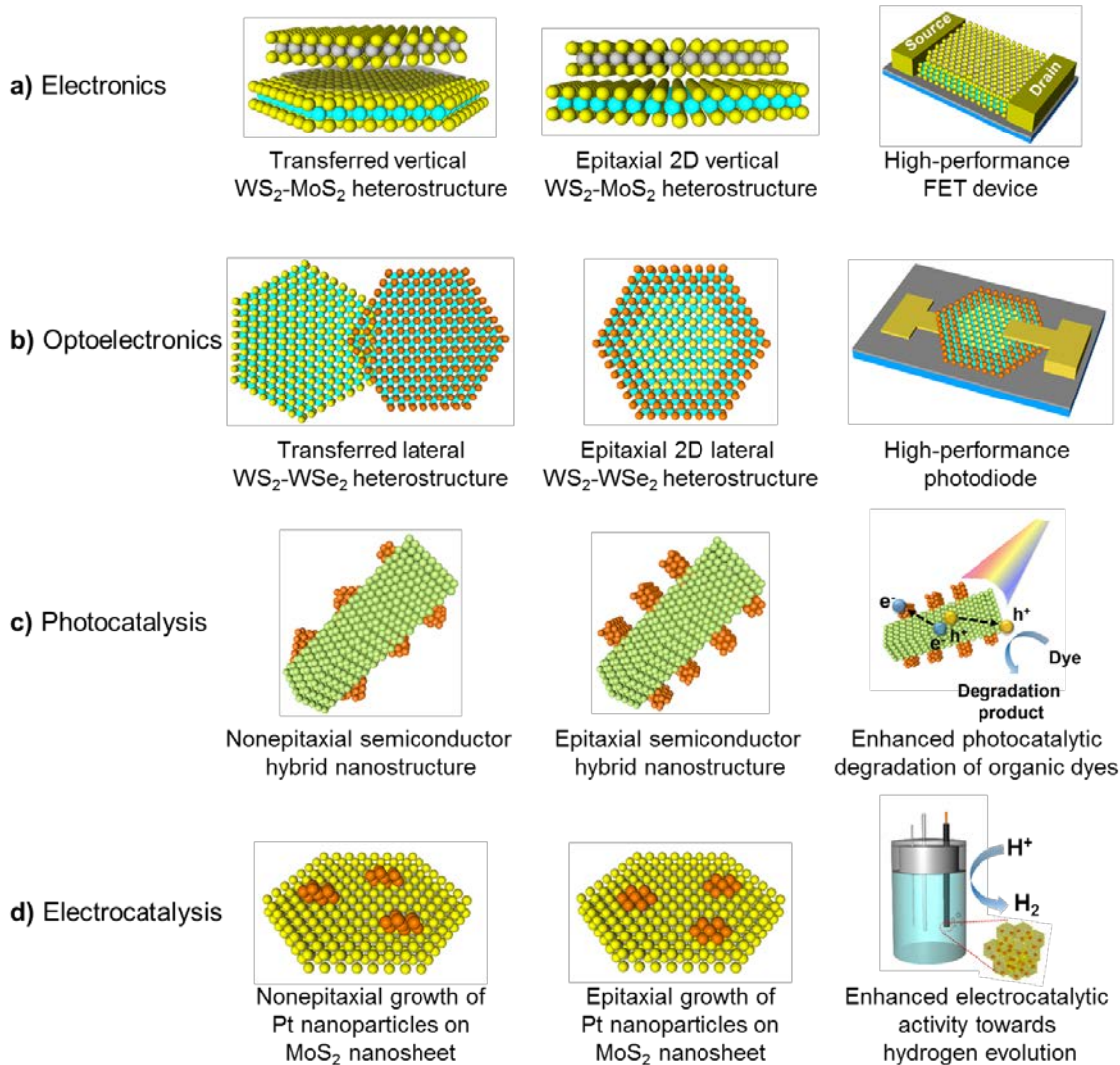


**Figure 4** | Schematic illustration of the advantages of epitaxial hybrid nanostructures in some applications. (a) Electronics: The epitaxial 2D vertical  $WS_2$ - $MoS_2$  heterostructures have a clean interface compared to the transferred vertical  $WS_2$ - $MoS_2$  heterostructures by polymer-assisted method and thus exhibited better performance when used as channel materials for the fabrication of FET transistors. (b) Optoelectronics: The epitaxial 2D lateral  $WS_2$ - $WSe_2$  heterostructures have a seamless interface compared to the transferred lateral  $WS_2$ - $WSe_2$  heterostructures by polymer-assisted method and thus exhibited better performance when used as active materials for the fabrication of photodiodes. (c) Photocatalysis: The epitaxial semiconductor hybrid nanostructures can ensure the faster electron transfer between the two components in the hybrid nanostructures and thus exhibited better higher photocatalytic activity when used as photocatalysts for

photocatalysis like photodegradation of methylene blue. (d) Electrocatalysis: The epitaxial growth of Pt nanoparticles can enable the exposure of high-index facets of Pt nanoparticles (e.g. {311} planes) and thus exhibited excellent catalytic activity toward the electrochemical hydrogen evolution.